Physica E 42 (2010) 1417–1424

Contents lists available at ScienceDirect

Physica E

journal homepage: www.elsevier.com/locate/physe

Green synthesis of gold and silver nanoparticles using *Hibiscus rosa sinensis*

Daizy Philip *

Department of Physics, Mar Ivanios College, Thiruvananthapuram 695 015, India

ARTICLE INFO

Article history:
Received 23 August 2009
Received in revised form
15 November 2009
Accepted 24 November 2009
Available online 5 December 2009

Keywords:
Hibiscus rosa sinensis
Biosynthesis
Gold nanoparticles
Silver nanoparticles

ABSTRACT

Biological synthesis of gold and silver nanoparticles of various shapes using the leaf extract of *Hibiscus rosa sinensis* is reported. This is a simple, cost-effective, stable for long time and reproducible aqueous room temperature synthesis method to obtain a self-assembly of Au and Ag nanoparticles. The size and shape of Au nanoparticles are modulated by varying the ratio of metal salt and extract in the reaction medium. Variation of pH of the reaction medium gives silver nanoparticles of different shapes. The nanoparticles obtained are characterized by UV–vis, transmission electron microscopy (TEM), X-ray diffraction (XRD) and FTIR spectroscopy. Crystalline nature of the nanoparticles in the fcc structure are confirmed by the peaks in the XRD pattern corresponding to (1 1 1), (2 0 0), (2 2 0) and (3 1 1) planes, bright circular spots in the selected area electron diffraction (SAED) and clear lattice fringes in the high-resolution TEM image. From FTIR spectra it is found that the Au nanoparticles are bound to amine groups and the Ag nanoparticles to carboxylate ion groups.

1. Introduction

The size, shape and surface morphology play a vital role in controlling the physical, chemical, optical and electronic properties of nanomaterials. Nanoparticles of noble metals are even used for the purification of water which is one of the essential enablers of life on earth [1]. Gold nanoparticles have been considered as important area of research due to their unique and tunable surface Plasmon resonance (SPR) and their applications in biomedical science including drug delivery, tissue/tumor imaging, photothermal therapy and immunochromatographic identification of pathogens in clinical specimens [2]. Integration of green chemistry principles to nanotechnology is one of the key issues in nanoscience research. Since the development of the concept of green nanoparticle preparation by Raveendran et al.[3], there has been growing need for environmentally benign metal-nanoparticle synthesis process that do not use toxic chemicals in the synthesis protocols to avoid adverse effects in medical applications. The inspiration for green chemistry and bioprocesses comes from nature through yeast, fungi, bacteria and plant extracts in the synthesis of biocompatible metal and semiconductor nanoparticles [4,5].

The work reported all over the world on the microorganisms and plants in the synthesis of Au nanoparticles has been reviewed by Mohanpuria et al.[6]. Coreander leaf-mediated synthesis of Au nanoparticles has been carried out by Narayanan and Sakthivel [7] and the reduction is reported to be complete in 12 h. Kasturi et al.[8] have reported the synthesis of silver and gold nanoparticles using purified apiin compound extracted from henna leaf. The use of edible mushroom and natural honey in the synthesis of Au and Ag nanoparticles have also been reported very recently [9,10]. The present study is a report on the aqueous synthesis of gold and silver nanoparticles of anisotropic and spherical shapes obtained by adjusting the concentrations of metal ions and hibiscus (*Hibiscus rosa sinensis*) leaf extract at ambient conditions. This is simple, cost-effective, stable for long time, reproducible and previously unexploited method to obtain a self-assembly of Au/Ag nanoparticles.

Hibiscus is a medicinal herb usually used effectively in native medicines against hypertension, pyrexia and liver disorder [11]. It blocks adipogenesis [12] and is also used to treat dandruff and stimulate hair growth. Living systems have been reported to receive non-enzymatic protection from lipid peroxidation by antioxidants such as tocopherol, ascorbic acid, β-carotene and uric acid found in large quantities in fruits and vegetables. Food antioxidants act as reducing agents, reversing oxidation by donating electrons and hydrogen ions [13]. Hibiscus leaf extract contains antioxidant compounds and is applicable to prevent atherosclerosis in humans via its anti-hyperlipidaemic effect and anti-LDL oxidation [14]. Hypoglycemic activity of this extract has also been reported [15]. Hibiscus leaf extract contains [16] proteins, vitamin C, organic acids (essentially malic acid), flavinoids and anthocyanins. The ability of hibiscus extract as a natural starch and sucrose blocker is found to lower starch and sucrose absorption when injested at reasonable doses [17] by inhibiting amylase which in turn an influence the glycemic load favourably. The antioxidant potential and anti-implantation activity of hibiscus extract were also studied [18,19]. Several plants like alalfa, lemon grass, geranium leaves, *Cinnamomum*

* Tel.: +91 471 2530887.
E-mail addresses: philipdaizy@yahoo.co.in, daizyp@rediffmail.com.

1386-9477/$ - see front matter © 2009 Elsevier B.V. All rights reserved.
doi:10.1016/j.physe.2009.11.081

camphora, tamarind, neem, Aloe vera, coriander and capsicum annum were used to synthesize metal nanoparticles [6–8,20–27]. The present paper describes for the first time, *Hibiscus rosa sinensis* leaf-mediated biosynthesis of gold and silver nanoparticles.

2. Experimental

Hibiscus leaf shown in Fig. 1 was washed several times with de-ionized water. 20 g of hibiscus leaf was finely cut and stirred with 200 mL de-ionized water at 300 K for 1 min and filtered to get the extract. The filtrate is used as reducing agent and stabilizer. $HAuCl_4 \cdot 3H_2O$ and $AgNO_3$ were procured from Sigma-Aldrich.

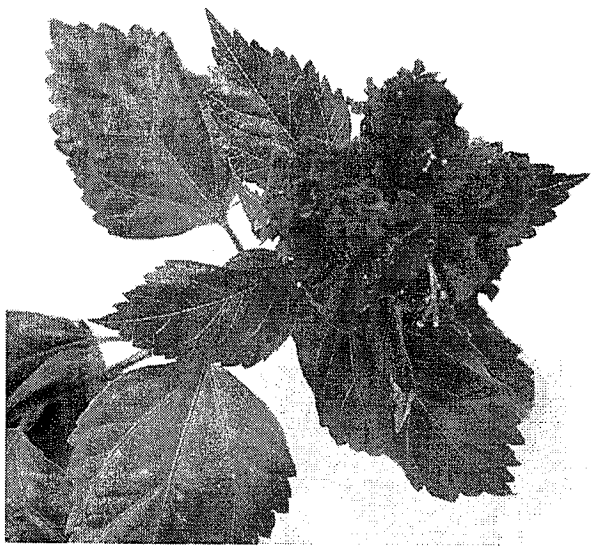

Fig. 1. Digital photograph of hibiscus leaf used in the synthesis.

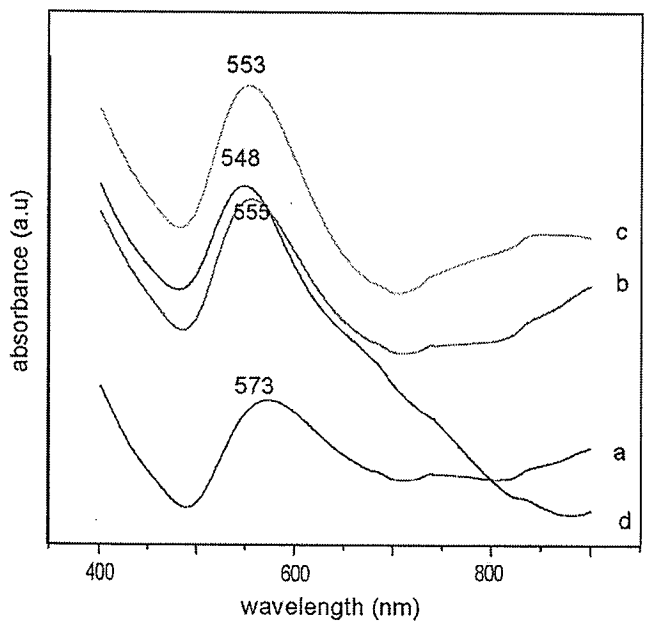

Fig. 2. UV–visible spectra of gold colloids: (a) g_1, (b) g_2, (c) g_3 and (d) g_4.

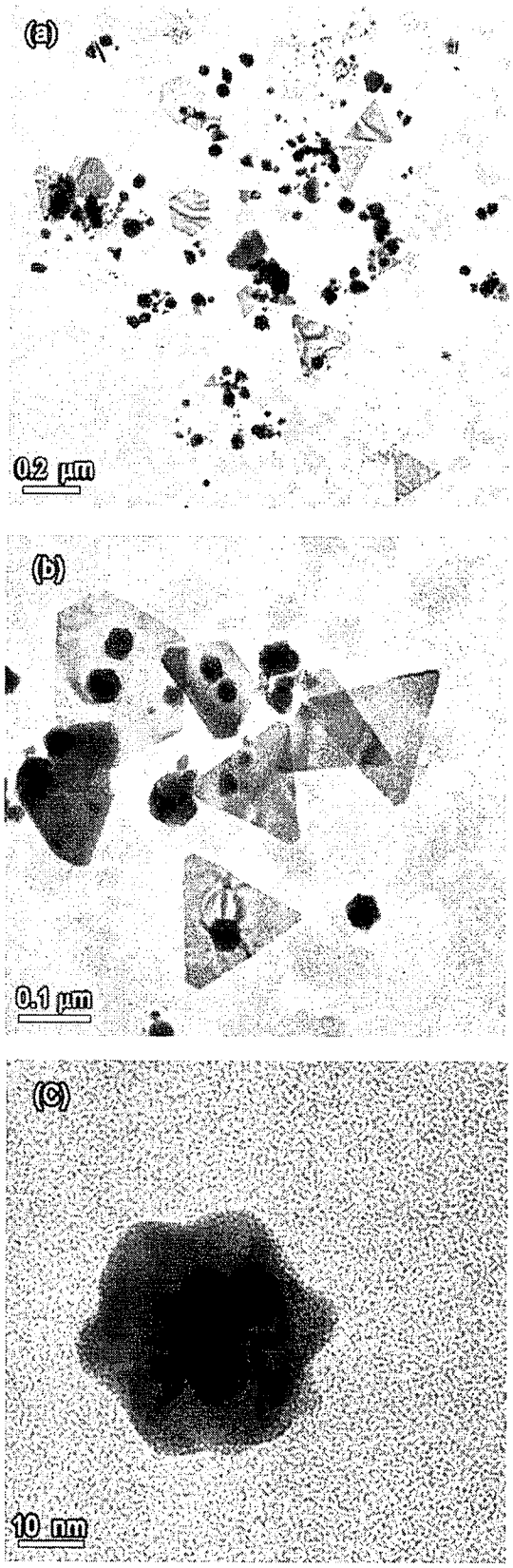

Fig. 3. TEM images of colloid g_2 (a) and (b) under different magnification; (c) single multi-branched gold nanoparticle.

2.1. Synthesis of gold nanoparticles

5 mL hibiscus extract is added to a vigorously stirred 30 mL aqueous solution of $HAuCl_4 \cdot 3H_2O$ (5×10^{-4} M) and stirring continued for 1 min. Slow reduction takes place and is complete in 1.5 h as shown by stable light violet colour of the solution which gives colloid g_1. To obtain colloids g_2, g_3 and g_4, the addition of the extract is varied as 10, 20 and 30 mL, respectively. It is found that reduction takes place rapidly with increase in addition of the extract and colloid g_4 is obtained in 30 min. The colloids are found to be stable for 2 months.

2.2. Synthesis of silver nanoparticles

20 mL hibiscus extract is added to a vigorously stirred 25 mL aqueous solution of $AgNO_3$ ($0.8 \times 10^{-}3$ M) and stirring continued for 1 min. To initialize the reduction of Ag ions, the pH of the solution is adjusted to be 6.8 using NaOH. Reduction takes place rapidly as indicated by golden yellow colour of the solution which gives colloid s_1. The colloids s_2, s_3, s_4, s_5 and s_6 are obtained by adjusting the pH of the solution to 7.2, 7.5, 7.8, 8.0 and 8.5. These colloids are found to be stable for 4 months.

The UV–visible spectra were recorded on a Jasco V-550 UV–visible spectrophotometer with samples in quartz cuvette. X-ray diffraction pattern of dry nanoparticle powder was obtained using Siemens D5005 X-ray diffractometer with CuK_α radiation (λ=0.1542 nm). The FTIR spectra were obtained on a Nicolet 5700 FTIR instrument with the sample as KBr pellets. The morphology of the nanoparticles was analysed using the high-resolution images obtained with a JEOL 3010 transmission electron microscope.

3. Results and discussion

3.1. UV–visible and TEM analysis of gold nanoparticles

UV–visible spectroscopy is an important technique to ascertain the formation and stability of metal nanoparticles in aqueous solution. Fig. 2 shows the UV–visible spectra of the gold colloids (g_1–g_4) obtained after 1.5 h of reaction. The colour of the colloid arises because of the surface plasmon vibrations with gold nanoparticles [28]. The surface Plasmon resonance (SPR) band of colloid g_1 occurs around 573 nm. The Plasmon bands of Au nanoparticles are broad with an absorption tail in the longer wavelength region that extends well into the near infrared region in colloids g_1, g_2 and g_3. This long wavelength absorption is attributed to the excitation of the longitudinal (in-plane) SPR and indicates significant anisotropy in the shape of gold nanoparticles. The band becomes narrower from g_1 to g_4 (Fig. 2) with a shift towards lower wavelength as the quantity of extract is increased. The fairly sharp SPR observed for colloid g_4 (Fig. 2(d)) at 548 nm is indicative of almost spherical nanoparticles. A similar result has been reported in gold nanoparticles synthesized using coriander leaf, apiin and edible mushroom [7–10].

The morphology and size of the synthesized nanoparticles were also determined by TEM images. Typical TEM images obtained for colloids g_2, g_3 and g_4 are shown in Figs. 3–5. The long wavelength tail in the SPR arising due to anisotropy of Au

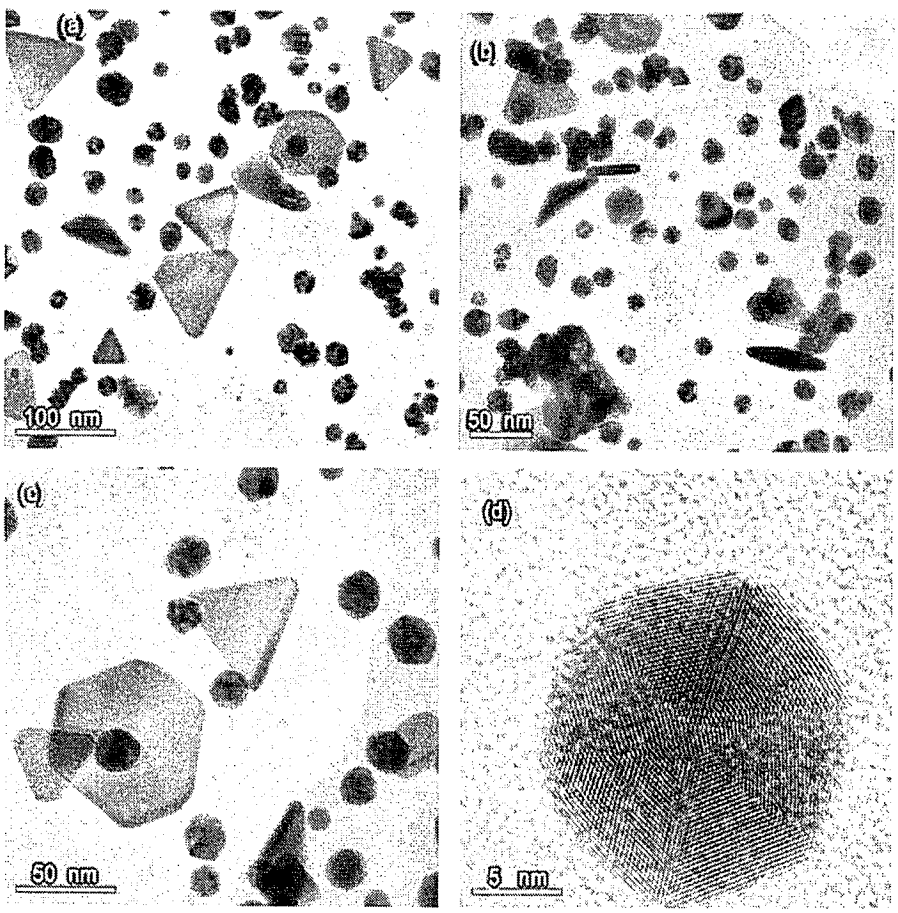

Fig. 4. TEM images of colloid g_3 (a)–(c) under different magnification; (d) single nanocrystal.

nanoparticles is evident from the TEM images of nanoparticles in colloids g_2 (Fig. 3) and g_3 (Fig. 4). Colloid g_2 consists of a large number of anisotropic particles with smaller ones being multi-branched (Fig. 3(c)). Nanoparticles with triangular, hexagonal, dodecahedral and spherical shapes are seen in g_3. The size and propensity of triangular particles decrease from colloid g_2 to g_4 and there is an increase in dodecahedral and spherical ones. In colloid g_4 (Fig. 5) the particles are almost spherical with size ~14 nm. The ability to modulate the shape of nanoparticles as observed in this study for Au nanoparticles opens up exciting possibility of further synthetic routes using biological sources. The typical high-resolution TEM image (Fig. 5(e)) with clear lattice fringes having a spacing of 0.23 nm reveals that the growth of Au nanoparticles occurs preferentially on the (1 1 1) plane. The inter-planar distance of the Au (1 1 1) plane is in agreement (29) with the (1 1 1) d-spacing of bulk Au (0.2355 nm). Fig. 5(f) shows the selected area electron diffraction (SAED) pattern of one of the spherical particles in colloid g_4. The clear lattice fringes in high-resolution TEM image and the typical SAED pattern with bright circular rings corresponding to the (1 1 1), (2 0 0), (2 2 0) and (3 1 1) planes show that the nanoparticles obtained are highly crystalline.

The decrease in intensity of the long wavelength tail of the SPR with increase in quantity of hibiscus extract and non-uniform dispersion of the nanoparticles may be explained as follows: When an excess of extract was used to reduce the aqueous

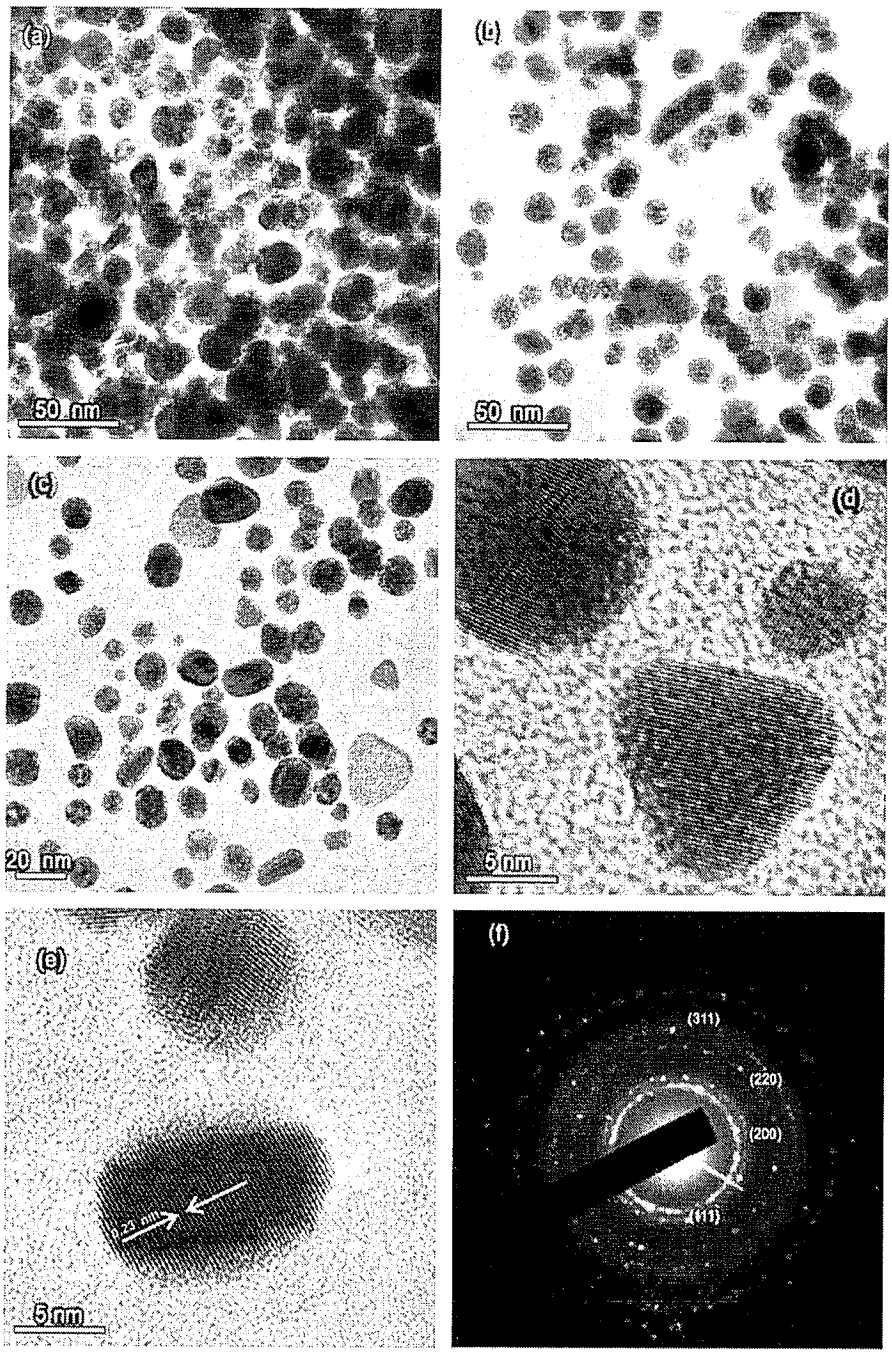

Fig. 5. TEM images of colloid g_4 (a)–(d) under different magnification; (e) single nanocrystal showing lattice fringes with spacing of 0.23 nm; (e) SAED pattern.

$HAuCl_4$, the biomolecules acting as capping agents strongly shaped spherical particles rather than nanotriangles, dodecahedral and hexagonal nanoparticles though the reductive biomolecules were enhanced [8–10]. Although lower quantities of the extract fulfilled the reduction of chloroaurate ions, they failed to protect most of the quasi-spherical nanoparticles from aggregating because of the deficiency of biomolecules to act as protecting agents. The nascent nanocrystals devoid of protection were unstable and gold nanotriangles and dodecahedrons might grow by a process involving rapid reduction, assembly and room temperature sintering of spherical gold nanoparticles [9,10,26]. Sintering of gold nanoparticles and their adherence to the nanotriangle is evident from Figs. 3(b) and 4(c). The formation of blunt-angled nanotriangles seen in the TEM images is a result of the shrinking process arising from the minimization of surface energy [9,10,26]. The presence of large quantity of extract causes strong interaction between protective biomolecules and surface of nanoparticles preventing nascent nanocrystals from sintering. With larger quantities of the extract the interaction is intensified, leading to size reduction of spherical nanoparticles. Similar results have been reported in biological synthesis of gold nanoparticles using apiin as reducing and stabilizing agent [8]. The present study also shows that in presence of a large quantity of the extract a uniform dispersion of spherical nanoparticles could be obtained.

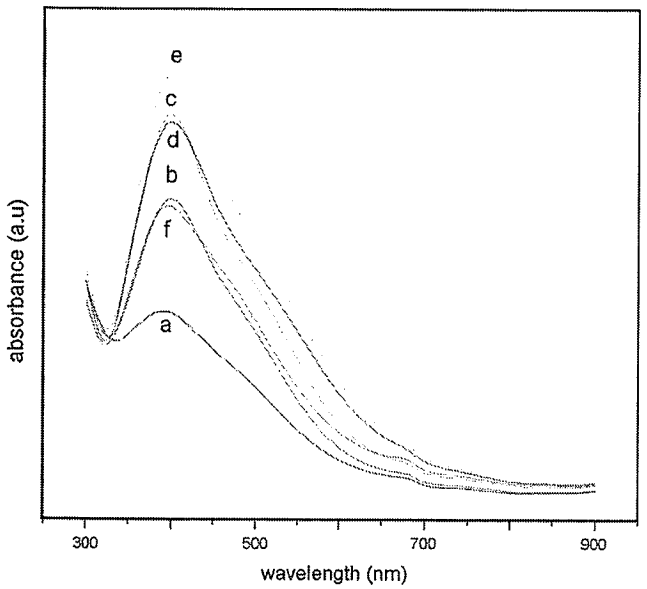

Fig. 6. UV–visible spectra of silver colloids (a) s_1, (b) s_2, (c) s_3, (d) s_4, (e) s_5 and (f) s_6.

3.2. *UV–visible and tem analysis of silver nanoparticles*

Fig. 6 shows the UV–visible spectra of silver nanoparticles formed at various pH values ranging from 6.8 to 8.5 of the reaction mixture consisting of aqueous $AgNO_3$ and hibiscus

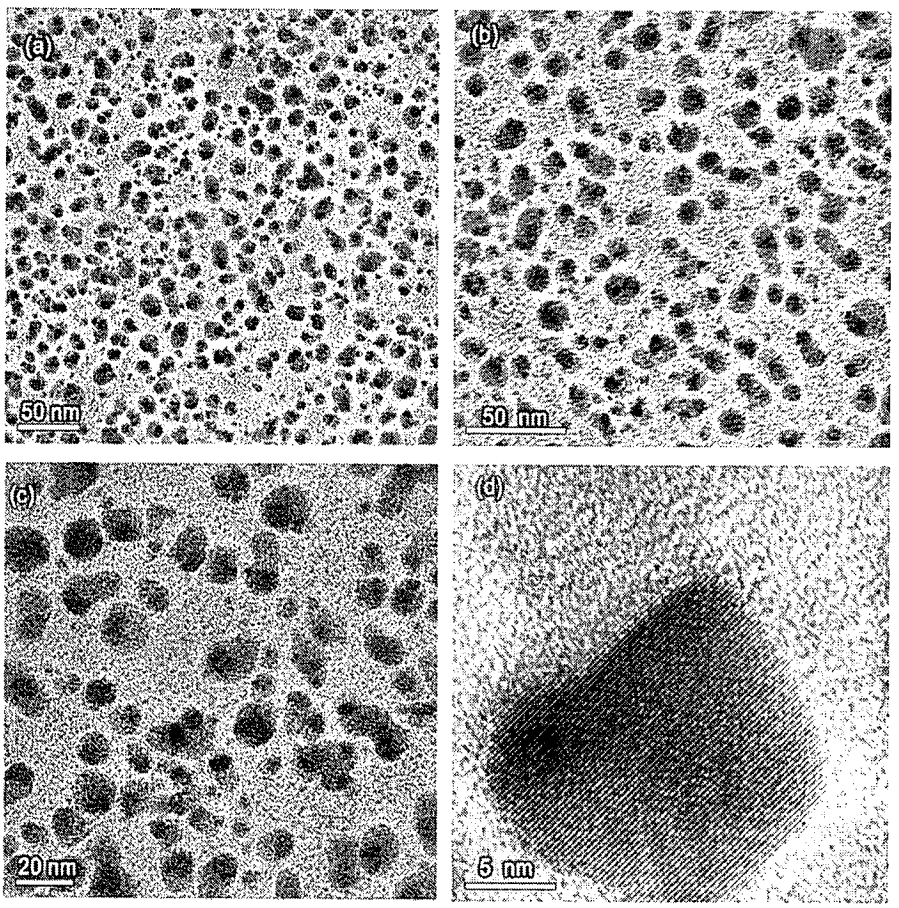

Fig. 7. TEM images of colloid s_3 (a)–(c) under different magnification; (d) single nanocrystal showing clear lattice fringes.

extract. The rapid colour change of the solution to golden yellow is indicative of the formation of silver nanoparticles. SPR band appears around 399 nm and becomes sharper as pH is increased upto 7.5 and thereafter it is broadened. The sharp SPR for s_3 indicating the formation of spherical nanoparticles is further confirmed by the TEM images in Fig. 7. Colloid s_3 consists of nearly spherical particles with an average size of ~13 nm. Crystallinity of silver nanoparticles is evidenced by the clear lattice fringes with a spacing of 0.23 nm (Fig. 7(d)). Broad SPR bands observed at higher and lower pH values are due to large anisotropic nanoparticles. Typical TEM images of anisotropic nanocrystals obtained for colloid s_6 are shown in Fig. 8. These anisotropic silver nanoparticles can act as suitable substrates for surface enhanced Raman scattering (SERS) spectroscopy using near IR (NIR) laser source.

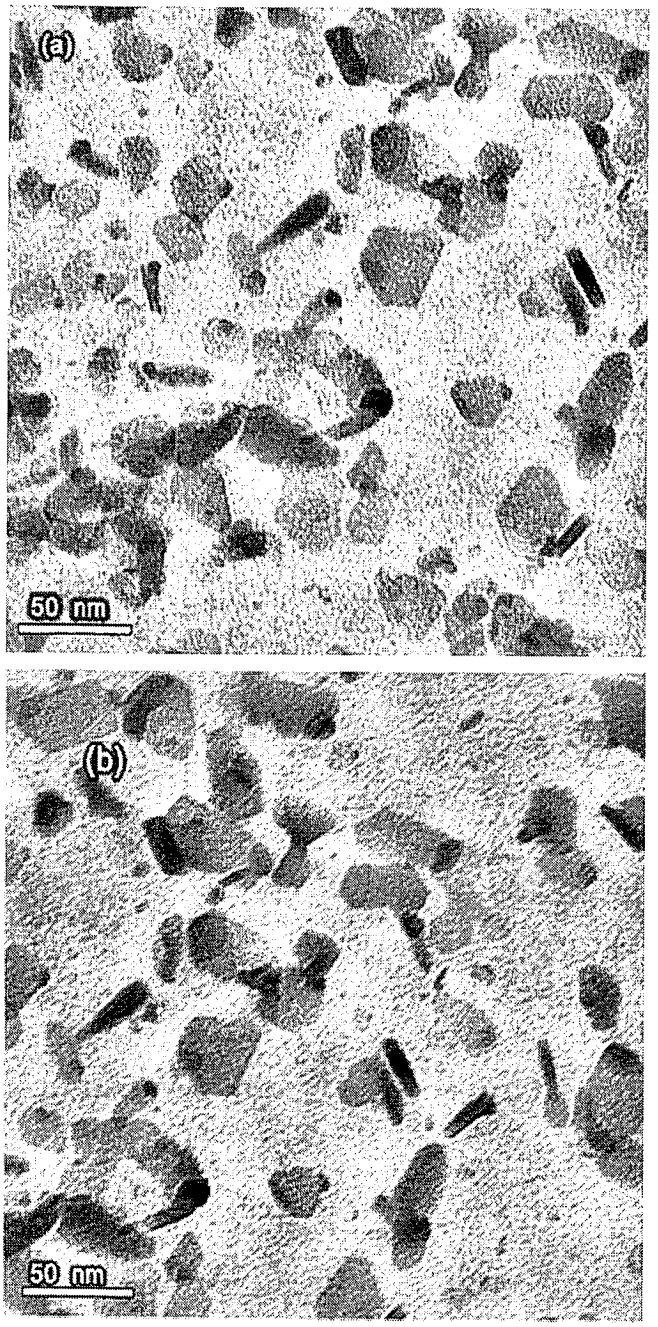

Fig. 8. TEM images of colloid s_6 (a) and (b) as viewed from different areas of the film.

3.3. XRD and FTIR studies

The crystalline nature of Au and Ag nanoparticles was further confirmed from X-ray diffraction (XRD) analysis. Fig. 9(a) shows the XRD pattern of the dried nanoparticles obtained from colloid g_4. Four peaks were observed at 38.2°, 44.3°, 64.7° and 77.8° in the 2θ range 30–80° which can be indexed to the (1 1 1), (2 0 0), (2 2 0) and (3 1 1) reflections of fcc structure of metallic gold, respectively (JCPDS no. 04-0784), revealing that the synthesized gold nanoparticles are composed of pure crystalline gold. The ratio between the intensity of the (2 0 0) and (1 1 1) diffraction peaks of 0.37 is lower than the conventional bulk intensity ratio (0.52), suggesting that the (1 1 1) plane is the predominant orientation as confirmed by high-resolution TEM measurements. Similar results were reported earlier in gold nanoparticles [9,10,29,30]. The average crystallite size according to Scherrer equation calculated using the width of the (1 1 1) peak is found to be 13 nm nearly in agreement with the particle size obtained from TEM image of colloid g_4. The XRD pattern of silver nanoparticles is shown in Fig. 9(b). In addition to the Bragg peaks representative of fcc silver nanocrystals, additional as yet unassigned peaks are also observed suggesting that the crystallization of bio-organic phase occurs on the surface of the silver nanoparticles. Similar results were reported in silver

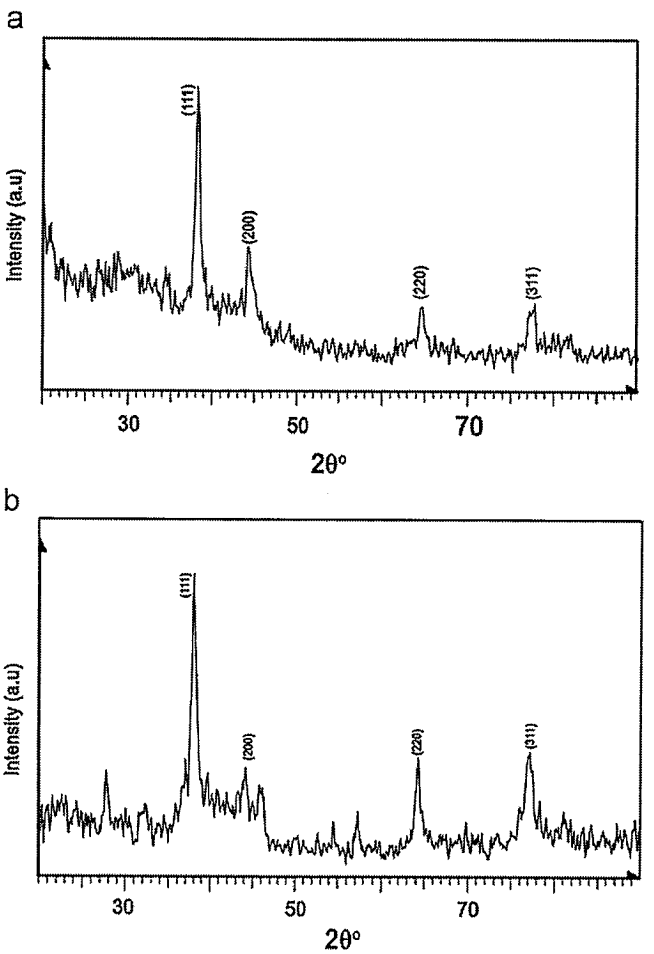

Fig. 9. XRD pattern of dried nanoparticle powder (a) gold and (b) silver.

nanoparticles synthesized using geranium leaf extract [22] and mushroom extract [9].

FTIR measurements were carried out to identify the potential biomolecules in hibiscus leaf responsible for reduction and capping of the bioreduced gold and silver nanoparticles. The IR bands (Fig. 10(a)) observed at 1317 and 1733 in dried hibiscus leaf are characteristic of the C–O and C=O stretching modes [7,9,22,31,32] of the carboxylic acid group possibly of malic acid present in it. The amide I band appears as very strong band at 1619 $cm^{-1}$and amide II band as a medium broad shoulder at 1546 cm^{-1} in the leaf. These amide I and II bands arise due to carboxyl stretch and N–H deformation vibrations in the amide linkages of the proteins [9,33–36] present in it. The medium broad band at 1399 cm^{-1} is the C–N stretching mode of aromatic amine group [7]. The C–O–C and C–OH vibrations [9,37] of the protein in the leaf appear as a very strong IR band at 1022 cm^{-1}.

The medium intense band at 1721 cm^{-1} is observed for the C=O stretching mode in the IR spectrum of gold nanoparticles (Fig. 10(b)) indicates the presence of –COOH group in the material bound to Au nanoparticles. However, in the spectrum of Ag nanoparticles (Fig. 10(c)), this mode is very weak or rather absent. Further, the band due to C–O stretching at 1314 cm^{-1} is intense in the spectrum of silver nanoparticles. The amide II band has become more prominent in the spectrum of gold and amide I band is shifted to higher frequency (1638 cm^{-1}) compared to that of plain leaf (1619 cm^{-1}). From these observations it is clear that the biomolecules responsible for reduction and capping are different in gold and silver nanoparticles. It is well-known that proteins can bind to Au nanoparticles through the free amine groups or carboxylate ion of aminoacid residue in it [31,34,38]. The presence of the IR bands due to C=O stretch at 1721 cm^{-1} and the prominent appearance of the amide I and amide II bands with large shift from that of the plain leaf indicate the possibility that gold nanoparticles are bound to proteins through free amine groups. Observation of almost unshifted positions of amide I and II bands compared to that of the plain leaf and the absence of C=O stretch of free –COOH in silver nanoparticles indicate the stabilization of the system through the $–COO^-$ (carboxylate ion) groups of aminoacid residues with free carboxylate groups in the protein [31,34,38]. However, the role of malic acid molecules present in the leaf extract on bioreduction and stabilization cannot be ruled out and needs further study as the band due to C–O stretch at 1314 cm^{-1} is appearing in the IR spectrum of silver nanoparticles.

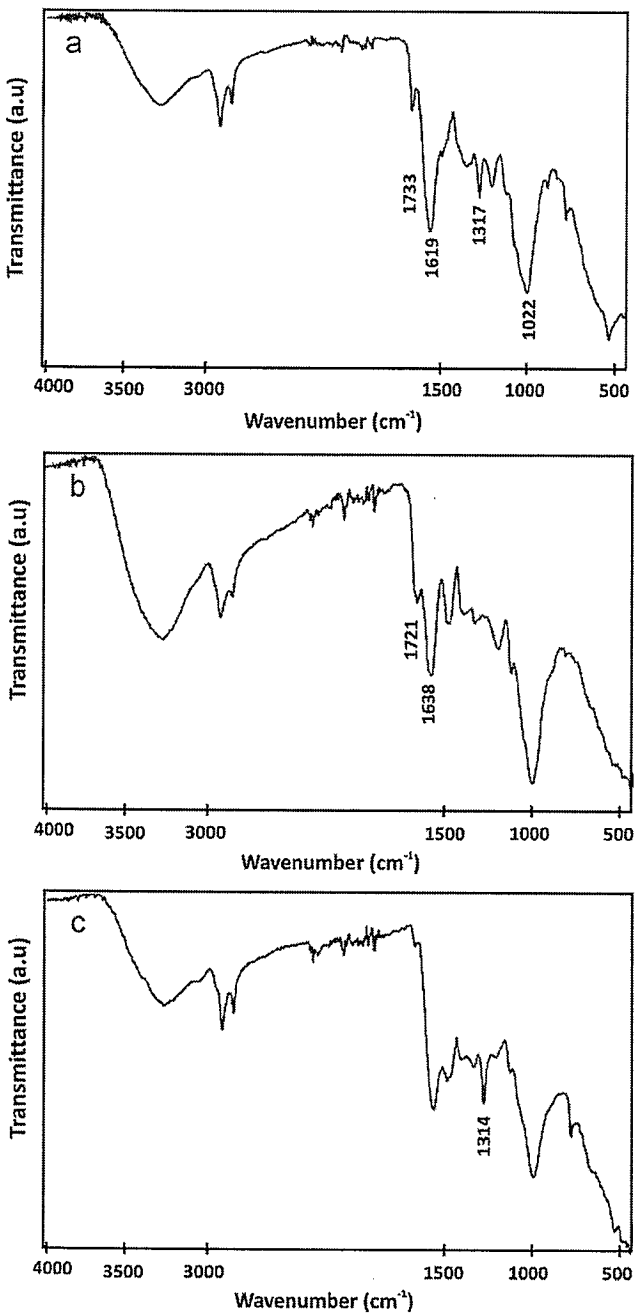

Fig. 10. FTIR spectra of (a) dried hibiscus leaf; dried powder of (b) gold nanoparticles and (c) silver nanoparticles.

4. Conclusions

Gold nanoparticles of different size and shape were synthesized using hibiscus leaf extract by varying the ratio of metal salt and the extract. Variation of pH of the reaction medium consisting of silver nitrate and hibiscus leaf extract gave silver nanoparticles of different shapes. The nanoparticles were characterized by UV–vis, TEM, XRD and FTIR measurements. Crystalline nature of the nanoparticles is evident from bright circular spots in the SAED pattern, clear lattice fringes in the high resolution TEM images and peaks in the XRD pattern. From FTIR spectra it is found that the stabilization occurs through amine groups in gold nanoparticles and carboxylate ion in silver nanoparticles.

Acknowledgements

This research has been sponsored by the University Grants Commission, New Delhi, under the Research Award scheme. The author is grateful to Professor T. Pradeep, DST unit on Nanoscience, IIT Madras for TEM measurements.

References

[1] T. Pradeep, Anshup, Thin Solid Films 517 (2009) 6441.
[2] S.H. Huang, Clin. Chim. Acta 373 (2006) 139.
[3] P. Raveendran, J. Fu, S.L. Wallen, J. Am. Chem. Soc. 125 (2003) 13940.
[4] S.S. Shankar, A. Ahmad, R. Parsricha, M. Sastry, J. Mater. Chem. 13 (2003) 1822.
[5] M.F. Lengke, M.E. Fleet, G. Southan, Langmuir 22 (2006) 2780.
[6] P. Mohanpuria, N.K. Rana, S.K. Yadav, J. Nanopart. Res. 10 (2008) 507.
[7] K.B. Narayanan, N. Sakthivel, Mater. Lett. 62 (2008) 4588.
[8] J. Kasturi, S. Veerapandian, N. Rajendran, Colloids Surf. B 68 (2009) 55.
[9] D. Philip, Spectrochim. Acta A 73 (2009) 374.

[10] D. Philip, Spectrochim. Acta A 73 (2009) 650.
[11] C.C. Chen, J.D. Hsu, S.F. Wang, H.C. Chiang, M.Y. Yang, E.S. Kao, Y.C. Ho, C.J. Wang, J. Agric. Food Chem. 51 (2003) 5472.
[12] M.S. Kim, J.K. Kim, H.J. Kim, S.R. Moon, B.C. Shin, K.W. Park, H.O. Yang, S.M. Kim, R. Park, J. Alter, Compl. Med. 9 (2003) 499.
[13] B. Halliwell, Nutr. Today 29 (1994) 15.
[14] P.S. Kang, J.H. Seok, Y.H. Kim, J.S. Eun, S.H. Oh, Food Sci. Biotechnol. 16 (2007) 409.
[15] A. Sachdewa, L.D. Khemani, J. Ethnopharmacol. 89 (2003) 61.
[16] H.A. Al-Kathani, B.H. Hassan, J. Food Sci. 55 (1990) 1073.
[17] H.G. Preuss, B. Echard, D. Bagchi, S. Stohs, Int. J. Med. Sci. 4 (2007) 196.
[18] M.M. Essa, P. Subramanian, T. Manivasagam, K.B. Dakshayani, R. Sivaperumal, S. Subash, Afr. J. Trad. Comp. Alt. Med. 3 (2006) 10.
[19] M. Nivsarkar, M. Patel, H. Padh, C. Bapu, N. Srivastava, Contracept 71 (2005) 227.
[20] V.K. Sharma, R.A. Yngard, Y. Lin, Adv. Colloid Interface Sci. 145 (2009) 83.
[21] J.L.G. Torresdey, E. Gomez, J.P. Videa, J.G. Parsons, H.E. Troiani, M.J. Yacaman, Langmuir 13 (2003) 1357.
[22] S.S. Shankar, A. Ahmad, M. Sastry, Biotechnol. Prog. 19 (2003) 1627.
[23] S.S. Shankar, A. Rai, B. Ankamwar, A. Ahmad, M. Sastry, Nat. Mater. 3 (2004) 482.
[24] S.P. Chandran, M. Choudhary, R. Paricha, A. Ahmad, M. Sastry, Biotechnol. Prog. 22 (2006) 577.
[25] S.S. Shankar, A. Rai, A. Ahmad, M. Sastry, J. Colloid Interface Sci. 275 (2004) 496.
[26] J. Huang, Q. Li, D. Sun, Y. Lu, Y. Su, X. Yang, H. Wang, Y. Wang, W. Shao, N. He, J. Hong, C. Chen, Nanotechnology 18 (2007) 105104.
[27] B. Ankamwar, C. Chinmay, A. Absar, M. Sastry, J. Nanosci. Nanotechnol. 10 (2005) 1665.
[28] P. Mulvaney, Langmuir 12 (1996) 788.
[29] P. Kannan, S.A. John, Nanotechnology 19 (2008) 085602.
[30] G.W. Jeong, Y.W. Lee, M. Kim, S.W. Han, J. Colloid Interface Sci. 329 (2009) 97.
[31] B. Ankamwar, M. Choudhary, M. Sastry, Synth. React. Inorg. Met. Nano. Chem. 35 (2005) 19.
[32] Z. Lin, J. Wu, R. Xue, Y. Yang, Spectrochim. Acta A 61 (2005) 761.
[33] S. Basavaraja, S.D. Balaji, A. Lagashetty, A.H. Rajasab, A. Venkataraman, Mater. Res. Bull. 43 (2008) 1164.
[34] A. Ahmad, S. Senapathi, M.I. Khan, R. Kumar, M. Sastry, Langmuir 19 (2003) 3550.
[35] S.S. Shankar, A. Ahmad, R. Pasricha, M.I. Khan, R. Kumar, M. Sastry, J. Colloid Interface Sci. 274 (2004) 69.
[36] T. Solomun, A. Shimanski, H. Sturm, E. Illenberger, Chem. Phys. Lett. 387 (2004) 312.
[37] S. Li, Y. Shen, A. Xie, X. Yu, X. Zhang, L. Yang, C. Li, Nanotechnology 18 (2007) 405101.
[38] J. Huang, Q. Li, D. Sun, Y. Lu, Y. Su, X. Yang, H. Wang, Y. Wang, W. Shao, N. He, J. Hong, C. Chen, Nanotechnology 18 (2007) 105104.